

# A universal ionization threshold for strongly driven Rydberg states

Andreas Krug\* and Andreas Buchleitner

Max-Planck-Institut für Physik komplexer Systeme, Nöthnitzer Str. 38, D-01187 Dresden

(Dated: January 3, 2019)

We observe a universal ionization threshold for microwave driven one-electron Rydberg states of H, Li, Na, and Rb, in an *ab initio* numerical treatment without adjustable parameters. This sheds new light on old experimental data, and widens the scene for Anderson localization in light matter interaction.

PACS numbers: 42.50.Hz, 05.45.Mt, 72.15.Rn

The suppression of quantum transport across disordered media is one of the most spectacular consequences of destructive quantum interference. Originally predicted by Anderson [1] in his treatment of electrons propagating in disordered one dimensional lattices, *Anderson localization* has now become a general concept which prevails in abundant scenarios of coherent quantum transport in the presence of disorder [2, 3]. Once it was realized that dynamical chaos has the potential to substitute disorder in the long time evolution of low dimensional systems on the classical as well as on the quantum level [4], it was natural to seek for a dynamical counterpart of Anderson localization in such a setting. Soon *dynamical localization*, i.e., the quantum suppression of diffusive energy growth in periodically driven, classically chaotic quantum systems was predicted [5, 6, 7] for the periodically kicked rotor and for microwave driven hydrogen atoms initially prepared in highly excited Rydberg states. Whilst experiments on cold atoms [8] – which closely mimic the kicked rotor in their center of mass motion – have confirmed this prediction in much detail, the situation remained controversial when it comes to the interpretation of experimental results on Rydberg states of atomic hydrogen and of alkaline atoms [9, 10, 11, 12, 13, 14, 15, 16, 17, 18]. There, the presence of additional degrees of freedom, of the atomic continuum, and of a multielectron atomic core prevent a direct mapping onto the Anderson picture, and considerably complicate the unambiguous interpretation of experimental results. On the other hand, such atomic systems obviously extend the potential realm of dynamical localization – i.e. of Anderson localization on the energy axis – considerably, since they provide generic examples of energy transport in light matter interaction.

In this Letter we present a unifying theoretical picture which, for the first time, resolves all apparent inconsistencies between experimental observations on different atomic species under microwave driving [9, 10, 12, 13, 18, 19]. On the basis of ample numerical data obtained from an accurate, approximation-free treatment of the atomic excitation and ionization process, we identify a scaling law under which the ionization thresholds of dif-

ferent atomic species coalesce for sufficiently high driving field frequencies, independently of their element specific, unperturbed spectral structure. This universality of the ionization threshold provides strong support for the Anderson scenario as the underlying transport mechanism, clearly beyond all evidence provided so far. Furthermore, it allows a purely spectral interpretation of the observed localization mechanism, irrespective of the availability of a well defined classical analogue.

Let us start with a condensed description of the physical system under study: In a typical laboratory experiment [9, 10, 13, 19], atomic one electron Rydberg states prepared in an initial field free state  $\rho_0$  are exposed to a classical monochromatic microwave field of frequency  $\omega$  and field strength  $F$ , for a duration  $t$  of typically several hundreds to several thousands of microwave periods  $T = 2\pi/\omega$ . After the atom field interaction, the percentage  $P_{\text{surv}}$  of atoms which did not ionize under the external driving is registered as a function of  $F$  and of the initial principal quantum number  $n_0$  which labels  $\rho_0$ . At fixed  $\omega$  and  $t$ , the ionization threshold field  $F(10\%)$  which induces  $1 - P_{\text{surv}} = 10\%$  is extracted from a series of such measurements, over a large interval of  $n_0$ . For a microwave frequency which is of the order of the local energy spacing  $\Delta E$  in the unperturbed Rydberg series, approx.  $N \simeq 1/2n_0^2\Delta E$  photons have to be absorbed by the atom to induce a transition from the initial state  $\rho_0$  into the atomic continuum, i.e. to produce a nonvanishing ionization signal. For typical values of  $n_0 \simeq 25 \dots 100$ , this implies multiphoton transitions of the order  $150 \dots 10$ , which can mediate efficient ionization only if they are composed of a sequence of near-resonant one photon transitions between Rydberg states separated by  $\omega \pm \delta$ , with small detuning  $\delta \ll \omega$ . The increasing density of states within the Rydberg progression towards the continuum threshold guarantees the existence of such a sequence, provided  $\omega$  is large enough to depopulate  $\rho_0$  via a first near resonant one photon transition. Under these premises, the intuitive analogy with the one dimensional Anderson model is established by identifying the sequence of near resonantly coupled Rydberg states with the neighbouring sites of a tight binding potential, with transition matrix elements essentially determined by the Rabi frequency which characterizes the one photon coupling. The one photon coupling constants are effectively randomized by the quasi ran-

---

\*present address: inuTech GmbH, Fürther Str. 212, D-90429 Nürnberg

dom distribution of detunings which is due to the non-linearity of the Rydberg progression to be set equal to  $m \times \omega$ , with integer  $m$  [20]. On the other hand, for  $\Delta E \sim n_0^{-3}$  – which defines the spacing of the degenerate energy levels of atomic hydrogen – the quantum mechanical transport process along the energy axis can be compared to classically chaotic transport in phase space, since  $\omega \sim n_0^{-3}$  defines strong nonlinear coupling between the unperturbed classical Kepler motion of the Rydberg electron and the external field, and hence leads to the efficient destruction of invariant tori in phase space for sufficiently large values of  $F$  [6, 7]. Given this classical picture of strongly driven Coulomb dynamics, the results of typical experiments on atomic hydrogen are most often represented in terms of scaled variables  $\omega_0 = \omega \times n_0^3$  and  $F_0(10\%) = F(10\%) \times n_0^4$ , what allows a direct identification of the experimental (quantum) result with the associated classical phase space structure which is completely determined by  $\omega_0$  and  $F_0$ . In such a plot, an increase of  $F_0(10\%)$  is considered as a signature of dynamical or Anderson localization, since classically diffusive/chaotic ionization leads to a monotonous decrease of  $F_0(10\%)$  with  $\omega_0$ , for not too short atom-field interaction times [18].

Despite the fact that no uniquely defined classical one particle dynamics is available for the excitation and ionization of nonhydrogenic initial states of alkaline Rydberg states, we compare in Fig. 1 the numerically generated scaled ionization thresholds of H, Li, Na, and Rb, as a function of  $\omega_0$ . The atoms are initially prepared in the low angular momentum state  $|n_0 \ell_0 = m_0 = 0\rangle$ , with  $\ell_0$  the angular momentum and  $m_0$  its projection on the polarization axis of the linearly polarized driving field. These results were obtained by diagonalization of the complex symmetric Floquet matrix which represents the complex dilated Floquet Hamiltonian of the driven atom, amended by the phase shift experienced by the electronic wave function of the Rydberg electron upon scattering from the multielectron core. Whilst details of our theoretical and numerical treatment can be found elsewhere [23, 25], let us just stress here that the atomic object under study is treated without any approximations on its dimensionality, that the atomic continuum is fully taken into account, and that no adjustable parameters are available. The results for the different species were obtained for fixed laboratory parameters  $\omega/2\pi = 36$  GHz and  $t = 327 \times T$ , and over a broad range  $28 \leq n_0 \leq 80$  of principal quantum numbers. Hence, representing the data in scaled units does not imply any a priori assumption on the relevant atomic energy scales, and the *only* possible cause of different ionization thresholds of different species is the element specific value of the nonvanishing quantum defects of the low angular momentum states.

Clearly, we can identify three regimes [25] in Fig. 1, which are defined by comparison of the hydrogen data with those for the nonhydrogenic alkaline initial states. In regime (I), at large scaled frequencies  $\omega_0 \geq 1$ , all

atomic species exhibit essentially *identical* ionization thresholds, *irrespective* of the specific structure of the unperturbed Rydberg spectra characterized by quite variable quantum defects ranging from 0 to 3.6, for  $\ell \leq 3$ . Only small relative differences on top of the general trend of the ionization threshold in this frequency regime reflect local spectral structures which differ from species to species and which determine the weight of individual atomic eigenstates in the field, in the decomposition of the initial field free state [11, 23, 24]. These differences are particularly pronounced for the experimental hydrogen data [9, 21] of the Stony Brook group also shown in this plot, since in these experiments (which, in addition, start from a statistical mixture  $\rho_0$  over the energy shell labelled by  $n_0$ ) the microwave is switched on rather slowly, allowing for a complicated sequence of (a)adiabatic transitions during the switching period of the microwave field. Notwithstanding, the global agreement of numerical and experimental data in regime (I) is rather impressive.

In regime (II), a strong discrepancy between the nonhydrogenic alkaline thresholds and those of atomic hydrogen develops as we proceed to smaller scaled frequencies, i.e. to smaller principal quantum numbers at fixed laboratory frequency [18, 21]. This sharp transition from (I) to (II) reflects the unavailability of a sequence of near resonant one photon transitions out of the hydrogen initial state quite dramatically, since the hydrogen threshold can take values larger by more than almost one order of magnitude as compared to the alkaline threshold. Remarkably, the alkaline thresholds still coalesce in this interval of principal quantum numbers, and the increase of  $F_0(10\%)$  with *increasing*  $\omega_0$  shows that the alkaline excitation and ionization process is still dominated by Anderson localization in this interval of scaled frequencies.

Only in regime (III) is the energy of the driving photon too small to couple one photon transitions in the alkaline species, and the threshold saturates accordingly (as a matter of fact, it slowly increases with decreasing scaled frequency, what is however barely realized on the scale of the figure – see [25] for an alternative presentation of the lithium data).

In the inset in Fig. 1, we compare the above ionization threshold of Rb at  $\omega/2\pi = 36$  GHz with the one at  $\omega/2\pi = 8.867$  GHz, within the same  $\omega_0$  interval and accordingly chosen values of  $n_0 = 59 \dots 80$ , at the same interaction time  $t = 327 \times T$ , and for a nonhydrogenic initial state with  $\ell_0 = 1$ . Clearly, both thresholds coincide in scaled units, with a small systematic shift of the  $\omega/2\pi = 8.867$  GHz results towards lower values, what is simply due to the systematically larger values of  $n_0$  imposed by the frequency scaling for the smaller laboratory value of the driving frequency [22]. Obviously, the classical scaling of frequency and amplitude cannot account for the semiclassical limit – which has to comply with the correspondence principle and hence must reproduce the classical ionization threshold which – by definition – is *smaller* than the quantum threshold in the Ander-

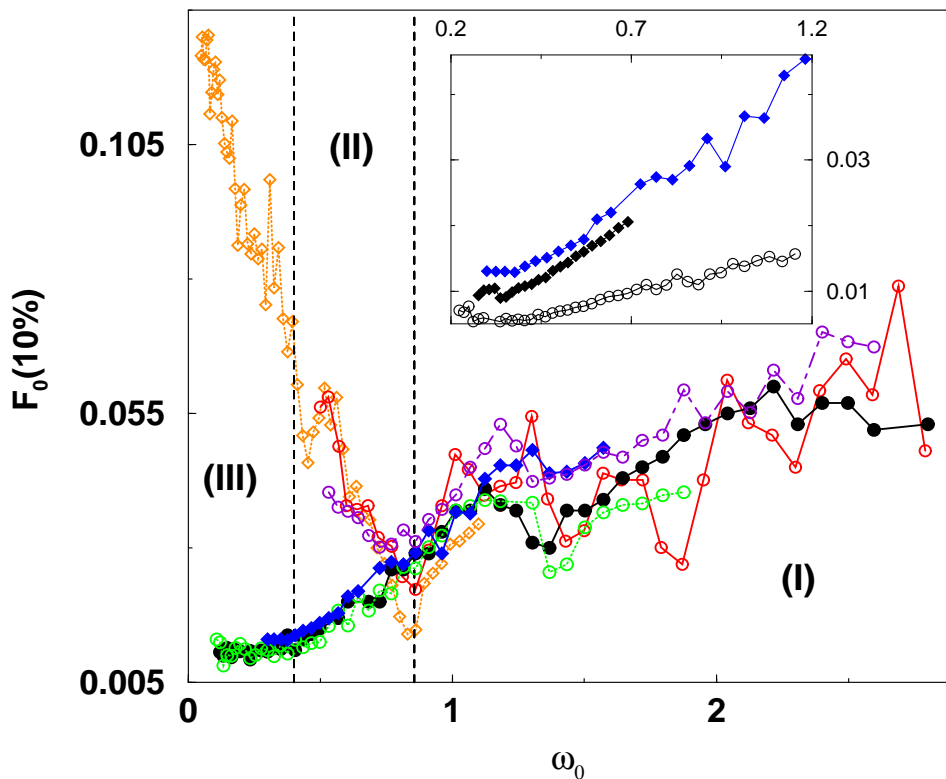


FIG. 1: Ionization thresholds of H (open diamonds, dotted line, and open circles, full line: laboratory experiments [9, 21]; open circles, dash-dotted line: numerical experiments), Li (filled circles, full line), Na (open circles, dotted line), and Rb (filled diamonds, full line), in scaled units  $\omega_0$  and  $F_0(10\%)$ . All data were obtained for an interaction time  $t = 327 \times T$ , at driving frequency  $\omega/2\pi = 36$  GHz, with initial principal quantum numbers in the range  $n_0 = 28 \dots 80$  except the ones represented by the open diamonds (here,  $\omega/2\pi = 9.95$  GHz, and  $n_0 = 32 \dots 90$  [21]). Hence, the comparison of alkali and hydrogen thresholds in scaled units does not imply any a priori assumption on the relevant atomic energy scales. Whilst all alkali data were obtained for *nonhydrogenic* initial states with angular momentum quantum numbers  $\ell_0 = 0$  and  $m_0 = 0$ , we observe a species-independent, universal ionization threshold in the high frequency range (I) – in strong support of the Anderson scenario as the dominant transport mechanism along the energy axis. Inset: Comparison of scaled Rb ionization thresholds, for driving frequencies  $\omega/2\pi = 36$  GHz,  $n_0 = 38 \dots 66$ ,  $\ell_0 = 0$  (filled triangles) and  $\omega/2\pi = 8.867$  GHz,  $n_0 = 59 \dots 80$ ,  $\ell_0 = 1$  (filled pyramids), respectively, at the same interaction time  $t = 327 \times T$ . Clearly, the scaled thresholds essentially coincide, except for a systematic shift of the 8.867 GHz data to slightly smaller threshold values. This is a consequence of approaching the semiclassical limit  $\hbar \sim n_0^{-1} \rightarrow 0$  whilst keeping the scaled frequency fixed [21, 22]. Also shown are experimental data (open circles) obtained at 8.867 GHz, though for much longer interaction times  $t = 44335 \times T$  [13]. Whilst the general  $\omega_0$  dependence is identical (notably the transition between frequency ranges (III) and (II)) for numerical and experimental data, the typically algebraic time dependence of the ionization threshold [13, 23] induces smaller thresholds for longer interaction times [19, 24].

son/dynamically localized regime.

The inset also contains experimental ionization thresholds of Rb  $\ell_0 = 1$  states under  $\omega/2\pi = 8.867$  GHz driving, though for much longer interaction times  $t = 44335 \times T$  [13]. Clearly, due to the nonvanishing decay rate of the eigenstates of the atom in the field, the experimentally observed ionization threshold is smaller than the numerical one obtained for shorter interaction times, but the transition between regimes (II) and (III) occurs in the same range at the same of  $\omega_0$  [23]! Furthermore, we see that the time dependence of the threshold is stronger for larger frequencies, thus slightly affecting the slope of the threshold curve – an observation also made in labora-

tory experiments on Li [19]. Indeed, a detailed study of the time dependence of the ionization threshold reveals a generic, algebraic decay law  $F_0(10\%) \sim t^{-\gamma}$ , where  $\gamma$  tends to increase slowly with  $\omega_0$  [23]. Whilst we could not reliably access the experimental regime of interaction times, since this requires extremely large a basis set such as to achieve numerical convergence of the decay rates better than  $10^{-13}$  a.u., typical values of  $\gamma$  are consistent with the gap opening up between the numerical and experimental 8.867 GHz data in Fig. 1 (note, however, that the precise value of  $\gamma$ , at a given value of  $n_0$  and  $\omega$ , will depend on the local spectral structure and on the particular envelope of the microwave pulse experienced by the

atoms [11, 24], which our numerical approach does not account for).

Given our observations in Fig. 1, the following picture emerges: Atomic one electron Rydberg states exhibit a universal ionization threshold if the tight binding picture sketched initially can be realized by a sequence of near resonant one photon transitions connecting the initial field free state to the atomic continuum [20]. Consequently, in regime (I), for  $\omega_0 \geq 1$ , i.e. for photon energies larger than the hydrogenic level spacing, alkaline atoms and atomic hydrogen exhibit identical thresholds and ignore the additional nonhydrogenic level structure provided by the nonvanishing quantum defects of the different species. Also for alkaline atoms the scaling law inherited from the classical Coulomb dynamics prevails, since the energy spacing between the nonhydrogenic initial state and the hydrogenic manifold exhibits the same dependence on the principal quantum number as the hydrogenic energy splitting [29]. Nonhydrogenic states of alkali atoms exhibit Anderson/dynamical localization in regime (II), in the absence of well defined classical one electron dynamics, simply due to the availability of a sequence of near resonant one photon transitions to the continuum. Note that in this regime this spectral sub-

structure is provided by the scattering of the electron from the atomic multielectron core which, on the scale of a typical Rydberg orbit in the energy range considered here, acts as a point scatterer [26]. Given the tremendous enhancement of the alkaline ionization yield as compared to atomic hydrogen in this parameter range, this represents the arguably most dramatic, directly observable signature of core scattering so far observed in a chaotic quantum system: here, core scattering reestablishes Anderson localization! As compared to the core scattering effect the nonvanishing time dependence of the ionization threshold is but a correction: even increasing the interaction time by a factor 10...100 does lower the threshold only weakly. All published experimental data which were so far interpreted in terms of dynamical localization were clearly obtained in regimes (II) and (III). The universal threshold in regime (I) was a theoretical prediction [23], which, however, has been confirmed in very recent laboratory experiments [27, 28] on one electron Rydberg states of Li and Sr.

Support as a Grand Challenge project at the Leibniz-Rechenzentrum of the Bavarian Academy of Sciences is most gratefully acknowledged.

- 
- [1] P. Anderson, Phys. Rev. **109**, 1492 (1958).  
 [2] D. S. Wiersma, P. Bartolini, A. Lagendijk, and R. Righini, Nature (London) **390**, 671 (1997).  
 [3] B. Kramer and A. MacKinnon, Rep. Prog. Phys. **56**, 1469 (1993).  
 [4] O. Bohigas, M. J. Giannoni, and C. Schmit, Phys. Rev. Lett. **52**, 1 (1984).  
 [5] S. Fishman, D. R. Grempel, and R. E. Prange, Phys. Rev. Lett. **49**, 509 (1982).  
 [6] G. Casati, B. V. Chirikov, and D. L. Shepelyansky, Phys. Rev. Lett. **53**, 2525 (1984).  
 [7] R. Blümel and U. Smilansky, Phys. Rev. Lett. **52**, 137 (1984).  
 [8] F. L. Moore, J. C. Robinson, C. Bharucha, P. E. Williams, and M. G. Raizen, Phys. Rev. Lett. **73**, 2974 (1994).  
 [9] E. J. Galvez, B. E. Sauer, L. Moorman, P. M. Koch, and D. Richards, Phys. Rev. Lett. **61**, 2011 (1988).  
 [10] J. E. Bayfield, G. Casati, I. Guarneri, and D. W. Sokol, Phys. Rev. Lett. **63**, 364 (1989).  
 [11] H. P. Breuer, K. Dietz, and M. Holthaus, J. Phys. B **22**, 3187 (1989).  
 [12] P. Fu, T. J. Scholz, J. M. Hettema, and T. F. Gallagher, Phys. Rev. Lett. **64**, 511 (1990).  
 [13] M. Arndt, A. Buchleitner, R. N. Mantegna, and H. Walther, Phys. Rev. Lett. **67**, 2435 (1991).  
 [14] R. Graham, Comm. At. Mol. Phys. **25**, 219 (1991).  
 [15] T. F. Gallagher, Comm. At. Mol. Phys. **25**, 159 (1991).  
 [16] P. Koch, L. Moorman, and B. Sauer, Comm. At. Mol. Phys. **25**, 165 (1991).  
 [17] S. Fishman and D. L. Shepelyansky, Europhys. Lett. **16**, 643 (1991).  
 [18] O. Benson, A. Buchleitner, G. Raithel, M. Arndt, R. N. Mantegna, and H. Walther, Phys. Rev. **A51**, 4862 (1995).  
 [19] M. W. Noel, W. M. Griffith, and T. F. Gallagher, Phys. Rev. A **62**, 63401 (2000).  
 [20] N. Brenner and S. Fishman, Phys. Rev. Lett. **77**, 3763 (1996).  
 [21] P. M. Koch and K. A. H. van Leeuwen, Phys. Rep. **255**, 289 (1995).  
 [22] A. Buchleitner, D. Delande, and J. C. Gay, J. Opt. Soc. Am. B **12**, 505 (1995).  
 [23] A. Krug, Ph.D. thesis, Ludwig-Maximilians-Universität München (2001), <http://edoc.ub.uni-muenchen.de/archive/00000336/>.  
 [24] A. Buchleitner, D. Delande, J. Zakrzewski, R. N. Mantegna, M. Arndt, and H. Walther, Phys. Rev. Lett. **75**, 3818 (1995).  
 [25] A. Krug and A. Buchleitner, Phys. Rev. A **66**, 53416 (2002).  
 [26] T. Jonckheere, B. Grémaud, and D. Delande, Phys. Rev. Lett. **81**, 2442 (1998).  
 [27] T. Gallagher, oral contribution, 296. WE-Heraeus-Seminar “Chaos and Quantum Transport”, Bad Honnef, 23-27 March 2003.  
 [28] H. Maeda and T. Gallagher (2004), preprint.  
 [29] As a matter of fact, this scaling law also allows to understand experimental data on Rb at  $\omega/2\pi = 12.6$  GHz [18], where a prominent enhancement of the ionization threshold was observed at  $n_0 = 89$ , though could not be explained: In Coulomb scaling, this corresponds to a scaled frequency  $\omega_0 \simeq 1.3$ , and the local maximum of  $F_0(10\%)$  thus is a remnant of the principal nonlinear resonance island in the classical phase space of the driven two-body system [21].